Inorg. Chem. **2006**, *45*, 9826–9833

Extremely Long Axial Cu–N Bonds in Chiral One-Dimensional Zigzag Cyanide-Bridged Cu^{II}–Ni^{II} and Cu^{II}–Pt^{II} Bimetallic Assemblies

Takashiro Akitsu* and Yasuaki Einaga

Department of Chemistry, Faculty of Science and Technology, Keio University, 3-14-1 Hiyoshi, Kohoku-ku, Yokohama, Kanagwa 223-8522, Japan

Received May 9, 2006

Preparations, crystal structures, and spectral and magnetic properties of two new chiral one-dimensional cyano-bridged coordination polymers, $[Cu^{II}L_2][M^{II}(CN)_4]\cdot 2H_2O$ (M^{II} = Ni^{II} (**1**) and Pt^{II} (**2**), L = *trans*-cyclohexane-(1*R*,2*R*)-diamine) have been presented. Complex **1** crystallizes in the monoclinic $P2_1$ space group with a = 9.864(4) Å, b = 15.393(8) Å, c = 7.995(4) Å, β = 110.32(3)°, V = 1138.4(10) Å^3, and Z = 2, while **2** crystallizes in the monoclinic $P2_1$ space group with a = 9.899(3) Å, b = 15.541(4) Å, c = 8.102(2) Å, β = 111.02(2)°, V = 1163.6(5) Å^3, and Z = 2. The unique zigzag cyano-bridged chains along the crystallographic b axis consist of alternate chiral $[CuL_2]^{2+}$ cations and square-planar $[M(CN)_4]^{2-}$ anions. One side of the axial Cu–N(≡C) bond distances are 2.324(6) and 2.34(1) Å with Cu–N≡C angles of 137.8(6)° and 138.2(9)° for **1** and **2**, respectively. On the other hand, the opposite side of the axial Cu–N(≡C) bond distances are 3.120(8) and 3.09(1) Å with significantly large bent Cu–N≡C angles of 97.9(5)° and 96.8(7)° for **1** and **2**, respectively. The novel axial bonding features of extremely long semi-coordination Cu–N bonds are attributed to coexistence of pseudo-Jahn–Teller elongation and electrostatic interaction in the unique zigzag cyano-bridged chains. The characteristic bonding features with overlap between small 3d (Ni^{II}) or large 5d (Pt^{II}) and 3d (Cu^{II}) orbitals results in larger shifts in XPS peaks of not only $Cu2p_{1/2}$ and $Cu2p_{3/2}$ but also $Ni2p_{1/2}$ and $Ni2p_{3/2}$ for **1** than those of **2**, which is also consistent with weak antiferromagnetic interactions with Weiss constants of –5.31 and –5.94 K for **1** and **2**, respectively. The d–d, π–π^*, and CT bands in the electronic, CD, and MCD spectra for **1** and **2** in the solid state at room temperature are discussed from the viewpoint of magneto-optical properties.

Introduction

Recently, there has been tremendous interest in functional as well as synthetic design of coordination polymers based on crystal engineering.[1,2] In particular, the development of cyano-bridged bimetallic assemblies has been widely employed for multidimensional organic−inorganic coordination polymers as molecule-based magnets.[3,4] This fact has created important expectations in the search for new materials that possess not only expected properties with conventional dimensionality but also multifunctionality, for instance, photomagnets[5,6] and chiral magnets.[7−13] Some of the most famous photomagnets may be Fe−Co Prussian blue analogues, [14] which are three-dimensional arrays of cyano-bridged inorganic solids showing photoinduced electron transfer[15,16] and lattice strain to weaken the ligand field of

* To whom correspondence should be addressed. Phone: +81-45-566-1790. Fax: +81-45-566-1697. E-mail: akitsu@chem.keio.ac.jp.

(1) Braga, D. *Chem. Commun.* **2003**, 3751.
(2) Braga, D.; Brammer, L.; Champness, N. R. *CrystEngComm.* **2005**, *7*, 1.
(3) Ohba, M.; Okawa, H. *Coord. Chem. Rev.* **2000**, *198*, 313.
(4) Okawa, H.; Ohba, M. *Bull. Chem. Soc. Jpn.* **2002**, *75*, 1191.
(5) Sato, O. *Acc. Chem. Res.* **2003**, *36*, 692.
(6) Sato, O.; Hayami, S.; Einaga, Y.; Gu, Z.-Z. *Bull. Chem. Soc. Jpn.* **2003**, *76*, 443.
(7) Coronado, E.; Gimenez-Saiz, C.; Martinez-Agudo, J. M.; Neuz, A.; Romero, F. M.; Htoeckli-Evans, H. *Polyhedron* **2003**, *22*, 2435.
(8) Coronado, E.; Gimenez-Saiz, C.; Sanchez, V.; Neuz, A.; Romero, F. M. *Eur. J. Inorg. Chem.*. **2003**, 4289.
(9) Coronado, E.; Gomez-Garcia, C. J.; Nuez, A.; Romero, F. M.; Rusanov, E.; Stoeckli-Evans, H. *Inorg. Chem.* **2002**, *41*, 4615.
(10) Imai, H.; Inoue, K.; Kikuchi, K.; Yoshida, Y.; Ito, M.; Sunahara, T.; Onaka, S. *Angew. Chem., Int. Ed.* **2004**, *43*, 5618.
(11) Inoue, K.; Kikuchi, K.; Ohba, M.; Okawa, H. *Angew. Chem., Int. Ed.* **2003**, *42*, 4810.
(12) Inoue, K.; Imai, H.; Ghalsasi, P. S.; Kikuchi, K.; Ohba, M.; Okawa, H.; Yakhmi, J. V. *Angew. Chem., Int. Ed.* **2001**, *40*, 4242.
(13) Kumagai, H.; Inoue, K. *Angew. Chem., Int. Ed.* **1999**, *38*, 1601.
(14) Sato, O.; Iyoda, T.; Fujishima, A.; Hashimoto, K. *Science* **1996**, *272*, 704.
(15) Nishino, M.; Yoshioka, Y.; Yamaguchi, K. *Chem. Phys. Lett.* **1998**, *297*, 51.

10.1021/ic060783a CCC: $33.50 © 2006 American Chemical Society
Published on Web 10/31/2006

cyanide ligands.[17] In addition, new photomagnets of Nd−Fe/Co 3d−4f bimetallic assemblies[18,19] do not exhibit photoinduced electron transfer but structural changes around cyano bridges after light irradiation. Therefore, structural distortion (with or without phase transition) of cyano-bridged coordination polymers may provide the control and flexibility necessary to assemble solids with potentially tunable properties. With the aid of crystal engineering, introduction of so-called 'Jahn−Teller switching' of Cu^{II} moieties into coordination polymers may be a new strategy for structural strain-driven switching materials.[20−22] Low dimensionality may be useful for enhancing static structural distortion without phase transition in the solid state. As for one-dimensional bimetallic assemblies involving Cu^{II} moieties, $[Cu(en)_2][Ni(CN)_4]$,[23] $[Cu(en)_2][Pd(CN)_4]$,[24] and $[Cu(en)_2][Pt(CN)_4]$[25] complexes (en = ethylenediamine) are isostructural regardless of replacing metal elements. However, it has been reported that $[Ni(en)_2][Ni(CN)_4]$ and $[Ni(en)_2][Pd(CN)_4]$ complexes afford slightly *elongated* and *compressed* octahedral coordination geometries, respectively.[26] Even for a mononuclear complex, $[Cu(en)_2](ClO_4)_2$ exhibits thermally accessible and photoinduced structural changes with respect to Jahn−Teller elongated axial bonds.[27] As magnetochiral dichroism (linkage of both natural optical activity and magnetically induced Faraday effect) is expected,[28−35] chiral ligands play an important role as not only structural but also electronic factors. For example, structural regulation from mononuclear Cu^{II} complexes of both diasteromers[36,37] to clusters of chiral single-molecule nanomagnets[38,39] have been reported so far. Novel crystal structures of chiral space group, which are different from racemic ones, may be obtained using chiral ligands of one of the enantiomers. Herein, we describe the preparations, crystal structures, and spectral and magnetic properties of two new chiral one-dimensional cyano-bridged coordination polymers, $[Cu^{II}L_2][M^{II}(CN)_4]\cdot 2H_2O$ ($M^{II} = Ni^{II}$ (**1**) and Pt^{II} (**2**), L= *trans*-cyclohexane-(1*R*,2*R*)-diamine). Discussion will be focused on novel long axial bonds, namely, semi-coordination with ionic nature, and the related electronic properties.

Experimental Section

Materials. The precursor complex, $[CuL_2(H_2O)_2](NO_3)_2$, was prepared according to the literature method.[40] High-purity (98%) *trans*-cyclohexane-(1*R*,2*R*)-diamine (Aldrich) and the other reagents and solvents were commercially available and used as purchased without further purification.

Preparation of $[CuL_2][Ni(CN)_4]\cdot 2H_2O$ (1). Slow diffusion of an aqueous solution (10 mL) of $[CuL_2(H_2O)_2](NO_3)_2$ (0.1 mmol) onto an aqueous solution (10 mL) of $K_2[Ni(CN)_4]$ (0.1 mmol) gave rise to blue platelike single crystals at 298 K. Yield: 80.2%. Anal. Calcd for $C_{16}H_{32}CuN_8NiO_2$: C, 39.16; H, 6.57; N, 22.83. Found: C, 39.29; H, 6.74; N, 22.76. Mp 561 K (decomposition). IR (KBr, cm^{-1}): 1038s, 1125s, 1402s, 1442w, 1591s, 1637w, 2123s, 2134s, 2858s, 2925s, 3303m, 3433s.

Preparation of $[CuL_2][Pt(CN)_4]\cdot 2H_2O$ (2). Slow diffusion of an aqueous solution (10 mL) of $[CuL_2(H_2O)_2](NO_3)_2$ (0.1 mmol) onto an aqueous solution (10 mL) of $K_2[Pt(CN)_4]$ (0.1 mmol) gave rise to blue platelike single crystals at 298 K. Yield: 98.7%. Anal. Calcd for $C_{16}H_{32}CuN_8O_2Pt$: C, 30.64; H, 5.14; N, 17.87. Found; C, 30.30; H, 4.83; N, 18.10. Mp 556 K (decomposition). IR (KBr, cm^{-1}): 1034w, 1121w, 1375m, 1463s, 1632s, 2139m, 2167m, 2862m, 2876m, 2929s, 2957s, 3457s.

Physical Measurements. Elemental analyses (C, H, N) were carried out an Elementar Vario EL analyzer at Keio University. Infrared spectra were recorded as KBr pellets on a JASCO FT-IR 660 plus spectrophotometer in the range of 4000−400 cm^{-1} at 298 K. Thermal analysis was performed on a SHIMADZU DSC-60 differential scanning calorimeter (DSC), where the heating rate was 10 K min^{-1} in the range of 313−673 K. Diffuse reflectance electronic spectra were measured on a JASCO V-560 spectrophotometer equipped with an integrating sphere in the range of 850−220 nm at 298 K. Circular dichroism (CD) spectra and magnetic circular dichroism (MCD) spectra at 15 000 Oe were measured as KBr pellets on a JASCO J-720WI spectropolarimeter in the range of 900−200 nm at 298 K. X-ray photoelectron spectra (XPS) were recorded with a JEOL JPS-9000MX at 298 K. Powder samples were pressed as pellets and put under UHV to reach the 10^{-8} Pa range. The nonmonochromatized Mg Kα source was used at 10 kV and 10 mA as a flood gun to compensate for the nonconductive samples. The binding energy of the spectra was calibrated in relation to the C1s binging energy (284.0 eV), which was applied as an internal standard. The magnetic properties were investigated with a Quantum Design MPMS-XL superconducting quantum interference device magnetometer (SQUID) at an applied field 5000 Oe in a temperature range 2−300 K and 0−50 000 Oe at 2 and 5 K. Powder samples (39.18 and 38.91 mg for **1** and **2**, respectively) were measured in a pharmaceutical cellulose capsule. The apparatus signals and diamagnetic corrections were evaluated from Pascal's constants.

(16) Nishino, M.; Kubo, Yoshioka, Y.; Nakamura, A.; Yamaguchi, K. *Mol. Cryst. Liq. Cryst.* **1997**, *205*, 109.
(17) Escax, V.; Champion, G.; Arrio, M.-A.; Zacchigna, M.; Cartir dit Moulin, C.; Bleuzen, A. *Angew. Chem., Int. Ed.* **2005**, *44*, 4798.
(18) Li, G.; Akitsu, T.; Sato, O.; Einaga, Y. *J. Am. Chem. Soc.* **2003**, *125*, 12396.
(19) Li, G.; Sato, O.; Akitsu, T.; Einaga, Y. *J. Solid State Chem.* **2004**, *177*, 2835.
(20) Falvello, L. R. *J. Chem. Soc., Dalton Trans.* **1997**, 4463.
(21) Halcrow, M. A. *Dalton Trans.* **2003**, 4375.
(22) Kang, D.-B. *Bull. Korean Chem. Soc.* **2005**, *26*, 1965.
(23) Lokaj, J.; Syerova, K.; Sopkova, A.; Sivy, J.; Kettmann, V.; Vrabel, V. *Acta Crystallogr.* **1991**, *C47*, 2447.
(24) Cernak, J.; Skorsepa, J.; Abboud, K. A.; Meisel, M. W.; Orendac, M.; Orendacova, A.; Feher, A. *Inorg. Chim. Acta* **2001**, *326*, 3.
(25) Akitsu, T.; Einaga, Y. *Acta Crystallogr.* **2006** , *E62*, m862.
(26) Cernak, J.; Chomic, J.; Baloghova, D.; Dunaj-Jurco, M. *Acta Crystallogr.* **1988**, *C44*, 1902.
(27) Akitsu, T.; Einaga, Y. *Bull. Chem. Soc. Jpn.* **2004**, *77*, 763.
(28) Rikken, G. L. A.; Raupach, E. *Nature (London)* **1997**, *390*, 493.
(29) Rikken, G. L. A.; Raupach, E. *Nature (London)* **2000**, *405*, 932.
(30) Rikken, G. L. A.; Raupach, E.; Roth, T. *Physica* **2001**, *B294−295*, 1.
(31) Rikken, G. L. A.; Folling, J.; Wyder, P. *Phys. Rev. Lett.* **2001**, *87*, 236602.
(32) Rikken, G. L. A.; Strohm, C.; Wyder, P. *Phys. Rev. Lett.* **2002**, *89*, 133005.
(33) Rikken, G. L. A.; Raupach, E. *Phys. Rev.* **1998**, *E58*, 5081.
(34) Wang, Y.; Yu, J.; Du, Y.; Xu, R. *J. Solid State Chem.* **2004**, *177*, 2511.
(35) Kubota, M.; Arima, T.; Kaneno, Y.; He, J. P.; Yu, X. Z.; Tokura, Y. *Phys. Rev. Lett.* **2004**, *92*, 137401.
(36) Akitsu, T.; Komorita, S.; Urushiyama, A. *Bull. Chem. Soc. Jpn.* **2001**, *74*, 851.
(37) Akitsu, T.; Komorita, S.; Tamura, H. *Inorg. Chim. Acta* **2003**, *348*, 25.
(38) Domingo, N.; Gerbier, P.; Gomez, J.; Ruiz-Molina, D.; Amabilino, D. B.; Tejada, J.; Veciana, J. *Polyhedron* **2003**, *22*, 2355.
(39) Minguet, M.; Luneau, D. D.; Paulsen, C.; Lhotel, E.; Gorski, A.; Waluk, J.; Amabilino, D. B.; Veciana, J. *Polyhedron* **2003**, *22*, 2349.
(40) Pariya, C.; Liao, F.-L.; Wang, S.-L.; Chung, C.-S. *Polyhedron* **1998**, *17*, 547.

Table 1. Crystallographic Data for **1** and **2**

	1	**2**
formula	$C_{16}H_{32}CuN_8NiO_2$	$C_{16}H_{32}CuN_8O_2Pt$
fw	490.75	627.13
Space group	$P2_1$ (No. 4)	$P2_1$ (No. 4)
Z	2	2
a(Å)	9.864(4)	9.899(3)
b(Å)	15.393(8)	15.541(4)
c (Å)	7.995(4)	8.102(2)
β (deg)	110.32(3)	111.02(2)
V (Å^3)	1138.4(10)	1163.6(5)
ρ_{calcd} (g cm^{-3})	1.432	1.790
μ (mm^{-1})	1.788	6.945
unique reflns	2714	2692
R_1[a] [$I > 2\sigma(I)$]	0.0392	0.0278
R_w[b]	0.1049	0.0785
Flack parameter	0.01(3)	−0.009(13)

[a] $R_1 = \sum||F_o| - |F_c||/\sum|F_o|$. [b] $R_w = (\sum w(|F_o| - |F_c|)^2/\sum w|F_o|^2)^{1/2}$, $w = 1/(\sigma^2(F_o) + (0.1P)^2)$, where $P = (F_o^2 + 2F_c^2|)/3$.

X-ray Crystallography. Crystallographic data for **1** and **2** are summarized in Table 1. Blue platelike single crystals of **1** (0.30 × 0.30 × 0.10 mm) and **2** (0.50 × 0.20 × 0.20 mm) were glued on top of a glass fiber and coated with a thin layer of epoxy resin to measure the diffraction data. The X-ray intensities were measured at 297 K with graphite-monochromated Mo Kα radiation (λ = 0.71073 Å) on a Rigaku four-circle diffractometer AFC-7R. Completeness for **1** and **2** are 0.7505 and 0.9153, respectively. The structures were solved by direct methods using SIR 92[41] and expanded by Fourier techniques. The structures were refined on F^2 anisotropically for non-hydrogen atoms by full-matrix least-squares methods with SHELXL97[42] on a teXsan program package[43] on an SGI Indy workstation. Empirical absorption corrections were applied based on ψ scans. No significant decay in the intensity of three standard reflections was observed throughout the data collection. All non-hydrogen atoms were refined anisotropically. The hydrogen atoms were located at geometrically calculated positions with C−H = 0.950 Å and refined isotropically. Since hydrogen atoms could not be observed in the difference Fourier map, we could not introduce hydrogen atoms of water molecules connected to O1 and O2 atoms. Although residual electron density was also found in the difference Fourier maps, the models containing these peaks as water molecules resulted in an increase of R values. Therefore, we could not assign them nor discuss hydrogen bonds closely.

Results and Discussion

Description of the Structures. The molecular structure and crystal packing of **2** are shown in Figures 1 and 2, respectively. Selected bond distances and angles for **1** and **2** are summarized in Table 2.

The overall crystal structures of **1** and **2** are isostructural. The cell volume of **2** (1163.6(5) Å^3) is 2.17% larger than that of **1** (1138.4(10) Å^3) at 297 K, which is attributed to the difference in the ionic radii of Ni^{II} and Pt^{II} ions. We also investigated the unit cell parameters for **2** at 109 K, monoclinic, $P2_1$, a = 9.846(2) Å, b = 15.457(9) Å, c = 8.064(3) Å, β = 111.61(2)°, and V = 1148.80(77) Å^3, and

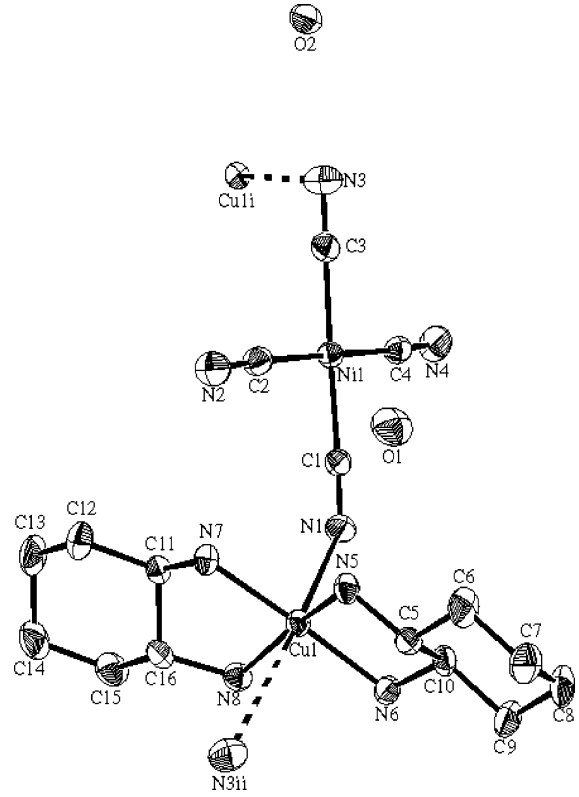

Figure 1. ORTEP drawing of the asymmetric unit of **2** showing the atom-labeling scheme. Displacement ellipsoids are drawn at the 30% probability level. Hydrogen atoms are omitted for clarity. [Symmetry codes: (i) $-x$, $1/2 + y$, $-z$; (ii) $-x$, $-1/2 + t$, $-z$].

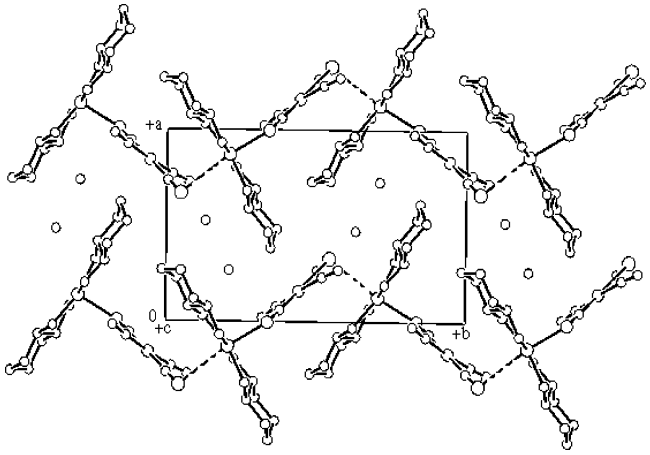

Figure 2. Packing diagram of **2** viewed from the c axis showing the one-dimensional zigzag chains. Hydrogen atoms are omitted for clarity.

Z = 2, and the thermally accessible cell volume change of **2** was only 1.27%. Therefore, this crystal lattice does not exhibit flexibility for thermally accessible structural changes. In contrast, mononuclear building block complexes are relatively flexible, and $[CuL_2(NO_3)_2]$ (in which L is the meso diastereomer of trans form) exhibit thermochromism or structural phase transition.[40]

Complexes **1** and **2** exhibit novel *zigzag* one-dimensional chain structures running along the crystallographic b axis. To emphasize the axial contacts for discussion, we show them like a normal bond in Figures 1 and 2. The heterome-

(41) Altomare, A.; Cascarano, G.; Giacovazzo, C.; Guagliardi, A.; Brurla, M. C.; Polidori, G.; Camalli, M. *J. Appl. Crystallogr.* **1994**, *27*, 435.
(42) Sheldrick, G. M. *SHELXL97, Program for the Refinement of Crystal Structures*; University of Gottingen: Germany, 1997.
(43) Molecular Structure Corp. *TEXSAN*, Version 1.11; MSC: The Woodlands, TX, 2001.

Table 2. Selected Bond Distances (Å) and Angles (deg) for **1** and **2**[a]

	1 (M = Ni)	**2** (M = Pt)
M1−C1	1.861(6)	2.000(8)
M1−C2	1.874(7)	1.99(1)
M1−C3	1.848(7)	2.006(9)
M1−C4	1.860(7)	1.97(1)
Cu1−N5	2.025(5)	2.007(7)
Cu1−N6	2.012(5)	2.020(8)
Cu1−N7	2.027(5)	2.019(9)
Cu1−N8	2.033(5)	2.022(8)
Cu1−N1	2.324(6)	2.34(1)
Cu1−N3^{ii}	3.120(8)	3.09(1)
C1−N1	1.142(9)	1.12(1)
C2−N2	1.135(10)	1.13(2)
C3−N3	1.161(9)	1.12(1)
C4−N4	1.151(10)	1.15(2)
C1−M1−C3	178.1(3)	177.8(4)
C2−M1−C4	176.3(3)	177.5(4)
N1−Cu−N3^{ii}	173.2(2)	171.8(3)
N5−Cu1−N8	166.1(2)	167.7(3)
N6−Cu1−N7	176.5(2)	176.8(3)
N5−Cu1−N6	84.6(2)	84.8(3)
N7−Cu1−N8	84.4(2)	83.5(3)
N5−Cu1−N7	94.2(2)	94.7(3)
N6−Cu1−N8	96.0(2)	96.3(3)
Cu1−N1−C1	137.8(6)	138.2(9)
Cu1^{i-}N3−C3	97.9(5)	96.8(7)
N3−C3−M1	176.1(7)	174(1)
N1−C1−M1	176.8(6)	175.8(10)

[a] Symmetry codes: (i) $-x, -1/2 + y, -z$. (ii) $-x, 1/2 + y, -z$.

tallic assemblies are formed by chiral $[CuL_2]^{2+}$ and square-planar $[M(CN)_4]^{2-}$ building blocks held together a bridging μ-CN groups in which two cyano groups in trans positions are used for bridging. Chiral ligands result in not only a noncentrosymmetric asymmetric unit but also structural regulation of the novel one-dimensional zigzag chains. In addition, formation of two- or three-dimensional structures is inhibited by bulky L ligands. In contrast to the present complexes, two-dimensional structures were reported for chiral complex $[Cu(R\text{-pn})_2][Ni(CN)_4]\cdot H_2O$ incorporating small *R*-pn (*R*-pn = *R*-1,2-diaminopropane) ligands.[44] Most of the geometric parameters for $[CuL_2]^{2+}$, $[Ni(CN)_4]^{2-}$, and $[Pt(CN)_4]^{2-}$ moieties are comparable to known related complexes such as $[CuL_2(H_2O)_2]Cl_2$,[40] $[Cu(en)_2][Ni(CN)_4]$,[23] $[Cu(en)_2][Pt(CN)_4]$,[25] and $[(CN)_3Pt(\mu\text{-CN})Cu(NH_3)_4]$.[45] In particular, six-membered cyclohexane rings of the L ligands are in trans chair−chair conformations for **1** and **2**.

It should be noted that interesting features could be found in extremely long axial semi-coordination Cu−N bonds for **1** and **2**. In accordance with the (pseudo) Jahn−Teller effect,[46] both sides of the axial Cu−N bond distances (Cu1−N1 and Cu1−N3^{ii}) are longer than those of the equatorial ones (Cu1−N5, Cu1−N6, Cu1−N7, and Cu1−N8) as shown in Table 2. One side of the axial bond distances (Cu1−N1) and Cu1−N1≡C1 bond angles are 2.324(6) Å and 137.8(6)° for **1** and 2.34(1) Å and 138.2(9)° for **2**. Regardless of the moderately bent Cu1−N1≡C1 bond angles, the Cu1−N1 bond distances can be considered as pseudo-Jahn−Teller distortion. On the other hand, the other side of the axial bond distances (Cu1−N3^{ii}) and Cu1^{i}−N3≡C3 bond angles, 3.120(8) Å and 97.9(5)° for **1** and 3.09(1) Å and 96.8(7)° for **2**, are apparently longer bond distances and larger bond angles than those for pseudo-Jahn−Teller distortion as described above. Using the conventional index of Jahn−Teller distortion, *T*, which is the ratio of equatorial Cu−N bond distances/axial Cu−N bond distances,[47] the degree of distortion of long (Cu1−N1) and short (Cu1^{i}−N3) axial bonds can be described to be $T = 0.649$ and 0.871 for **1** and $T = 0.653$ and 0.862 for **2**. Thus far, the longest axial Cu−N(≡C) bond distances and their thermal change have been reported to 2.394(7) Å at 102 K and 2.413(9) Å at 233 K for $[(CN)_3Pt(\mu\text{-CN})Cu(NH_3)_4]$.[45] It has been suggested that the significantly long axial bonds can be attributed to the contribution of ionic bonding characters. Furthermore, even for the largest data known for mononuclear $[Cu(en)_2](ClO_4)_2$ complex,[27] commonly the range of *T* values by thermally accessible structural changes are small, $T = 0.780$, 0.785, and 0.791 at 297, 274, and 120 K, respectively. Consequently, novel coexistence of pseudo-Jahn−Teller elongation and electrostatic interaction can be observed in both axial semi-coordination sites of the $[CuL_2]^{2+}$ moieties and cyanide-bridged chains for **1** and **2**. Intermolecular interactions in the solid state are not usually considered to have an important influence on molecular shape, which is determined principally by the stronger covalent and ionic bonds. Spectroscopic and magnetic properties will be mentioned in the succeeding sections.

The novel present case, in which two axial semi-coordination bonds are asymmetric, may have secondary bonds which occur in the electrically distorted Cu^{II} environment linked by predominantly strong electrostatic flux accompanying weak coordination bonds. The origin of the long-range force forming considerably weak bonds should be explained as follows: Polarization of the core electrons of the transition metal induces the second-order Jahn−Teller distortion of the one-dimensional cyanide-bridged metal−ligand chains with alternating long and short bonds being allowed by mixing filled orbitals on the Cu^{II} ion, namely, $3d_{z^2}$ in the chain direction, and cyanide ligands with the empty π^* orbitals.

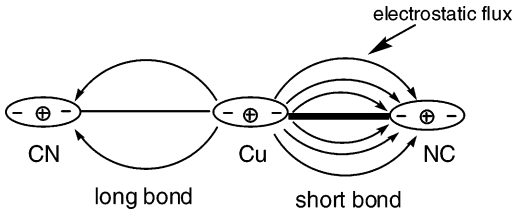

Possible hydrogen bonds can be proposed as follows: N5(−H5A)···O1^{iii} = 2.902(8) Å, O2···N3 = 2.797(8) Å, O1···O2^{iv} = 2.72(1) Å, N6(−H6A)···N4^{v} = 3.29(1) Å, N7(−H7C)···N4 = 3.24(1) Å, N7(−H7D)···N2 = 3.285(8) Å, N6(−H6B)···N2^{vi} = 3.12(1) Å, and N8(H8D)···O2 = 3.13(8) Å for **1** and N5(−H5B)···O1 = 2.91(1) Å, O2···N3 = 2.81(1) Å, O1···O2^{iv} = 2.68(1) Å, N6(−H6A)···N4^{v} = 3.34(1) Å, N7(−H7C)···N4 = 3.33(2) Å, N7(−H7D)···N2 =

(44) Imai, H.; Inoue, K.; Ohba, M.; Okawa, M.; Kikuchi, K. *Synth. Met.* **2003**, *137*, 919.
(45) Escorihuela, I.; Falvello, L. R.; Tomas, M. *Inorg. Chem.* **2001**, *40*, 636.
(46) Bersuker, I. B. *The Jahn−Teller Effect*; Cambridge University Press: Cambridge, U.K., 2006.
(47) Hathaway, B. J.; Billing, D. E. *Coord. Chem. Rev.* **1970**, *5*, 143.

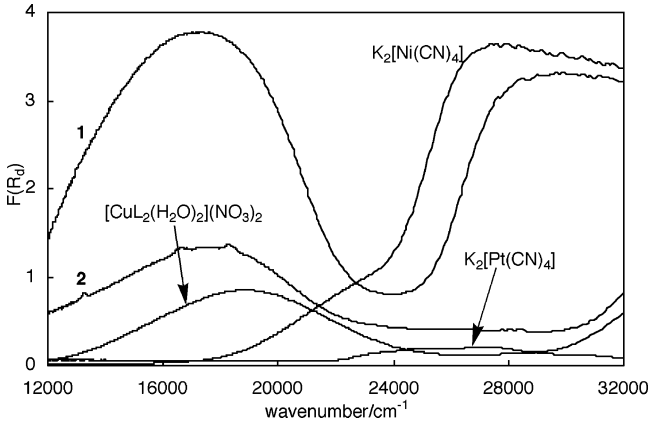

Figure 3. Diffuse reflectance electronic spectra for **1**, **2**, $[CuL_2(H_2O)_2](NO_3)_2$, $K_2[Ni(CN)_4]$, and $K_2[Pt(CN)_4]$ at 298 K.

3.35(1) Å, N6(−H6B)···N2^{vi} = 3.10(1) Å, and N8(H8D)···O2 = 3.02(1) Å for **2** [Symmetry code: (iii) $-x$, $y + 1/2$, $-z$, (iv) $1 - x$, $-1/2 + y$, $1 - z$, (v) $-x$, $-1/2 + y$, $-1 - z$, (vi) $-x$, $1/2 - y$, $2 - z$]. Hydrogen-bonding networks sometimes play an important role in magnetic interactions.[48] Because they are quite weak even through main cyano-bridged chains, their contribution can be negligible for **1** and **2**.

IR, Electronic, and CD/MCD Spectroscopies. The IR spectra exhibit sharp bands at 2123 and 2134 cm^{-1} for **1** and 2139 and 2167 cm^{-1} for **2**, which are attributed to C≡N stretching modes. The splitting into two bands is in agreement with the presence of two bridging and two nonbridging cyanide ligands at the trans sites.[49] However, the IR spectra could not distinguish between long and short bonding cyanide ligands. The spectral shifts between **1** and **2** are reasonable for metal substitution of Ni^{II} and Pt^{II} complexes.

Diffuse reflectance electronic spectra for **1**, **2**, $[CuL_2(H_2O)_2](NO_3)_2$, $K_2[Ni(CN)_4]$, and $K_2[Pt(CN)_4]$ at 298 K are depicted in Figure 3. In the visible region broad bands attributed to d−d transitions of Cu^{II} ions are at 17 500, 17 700, and 19 000 cm^{-1} for **1**, **2**, and $[CuL_2(H_2O)](NO_3)_2$, respectively. The spectral shift of the d−d bands between **1** (or **2**) and $[CuL_2(H_2O)](NO_3)_2$ is in agreement with replacement of axial ligands from cyanide with water.[50] The spectral difference between **1** and **2** can also support electronic interaction through the long bonds of the cyano bridges. In addition, **1** and $K_2[Ni(CN)_4]$ exhibit strong bands over about 28 500 cm^{-1} which can be assigned to symmetry-forbidden charge-transfer transition $2b_{1g} \rightarrow 4a_{2u}$ of $[Ni(CN)_4]^{2-}$ moieties.[51] However, emission spectra (λ_{ex} = 360 nm) for **1** and **2** could not be observed in the solid state at 298 K.

CD and MCD (at 15 000 G) spectra measured as KBr pellets at 298 K for **1** and **2** are depicted in Figure 4, which establish the enantiomeric character of the prepared coordination polymers and the structurally characterized ones. Because the measurement in the solid state was carried out at 298 K, the spectral information corresponds to diffuse reflectance electronic spectra (Figure 3) but does not correspond to magnetic measurements at low temperature (see a later section). The CD and MCD spectra for **2** are identical, while in **1** there is a clear difference. Since we measured the CD and MCD spectra in the solid state as KBr pellets at room temperature, the spectra did not reflect their magnetic interaction at low temperature. Because the intensity of the d−d bands in the visible region are weaker than CT and $\pi-\pi^*$ bands in the UV region, the spectra are extremely noisy and a distinct difference could not observed for **2** at this condition.

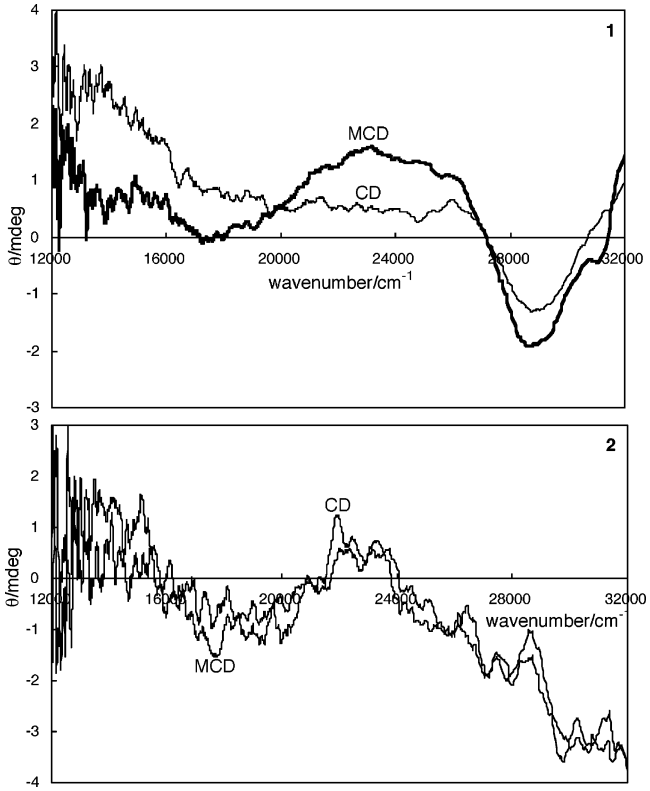

Figure 4. CD and MCD (15 000 G) for **1** and **2** as KBr pellets at 298 K.

Optical activity and the signs of the Cotton effect of **1** and **2** result from chiral L ligand (1*R*,2*R*) enantiomers as employed for preparation. Other typical chiral sources, such as helicity of the one-dimensional chains and Δ,Λ configurations of sterochemistry,[52,53] are not associated with the present complexes. The bands around 23 000 (positive Cotton effect) and 29 000 cm^{-1} (negative Cotton effect) are due to charge-transfer bands of $[Ni(CN)_4]^{2-}$ or $[Pt(CN)_4]^{2-}$ moieties, and the distinct and intense peak features of **1** are in agreement with the features of diffuse reflectance spectra in the similar wavenumber region. In addition, the similar signs of the Cotton effect for **1** and **2** in the same wavenumber region

(48) Zelenak, V.; Orendacova, A.; Cisarova, I.; Cernak, J.; Krachyna, O. V.; Park, J.-H.; Orendac, M.; Anders, A. G.; Feher, A.; Meisel, M. W. *Inorg. Chem.* **2006**, *45*, 1774.
(49) Kuchar, J.; Cernak, J.; Mayerova, Z.; Kubacek, P.; Zak, Z. *Solid State Phenomena* **2003**, *90*−*91*, 323.
(50) Walsh, A.; Hathaway, B. J. *J. Chem. Soc., Dalton Trans.* **1984**, 15.
(51) Mantz, Y. A.; Musselman, R. L. *Inorg. Chem.* **2002**, *41*, 5770.
(52) Andres, R.; Brissard, M.; Gruselle, M.; Train, C.; Vaissermann, J.; Malezieux, B.; Hamet, J.-P.; Verdaguer, M. *Inorg. Chem.* **2001**, *40*, 4633.
(53) Wen, H.-R.; Wwang, C.-F.; Song, Y.; Zuo, J.-L.; You, Z.-Z. *Inorg. Chem.* **2005**, *44*, 9039.

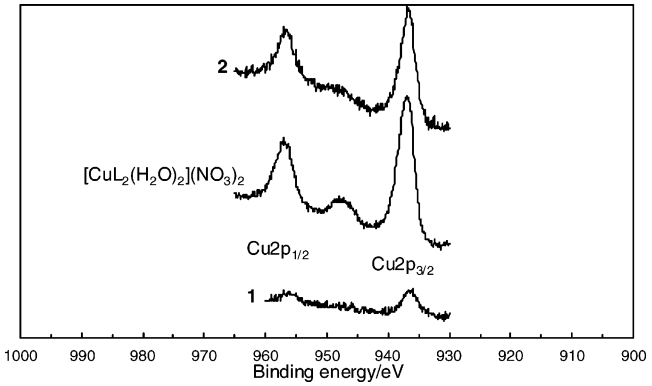

Figure 5. XPS spectra of $Cu2p_{1/2}$ and $Cu2p_{3/2}$ peaks for **1**, **2**, and $[CuL_2(H_2O)_2](NO_3)_2$, at 298 K.

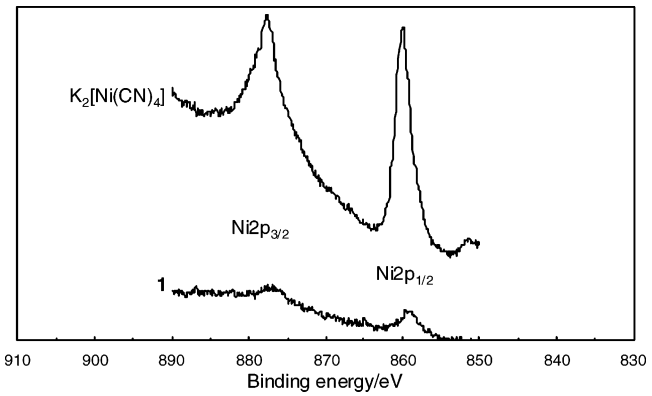

Figure 6. XPS spectra of $Ni2p_{1/2}$ and $Ni2p_{3/2}$ peaks for **1** and $K_2[Ni(CN)_4]$ at 298 K.

are attributed to the two chiral coordination polymers having the same absolute configuration.

XPS. In this paper, we plotted the intensity of XPS spectra in arbitrary unit scale. Each XPS in the range 0−1000 eV at 298 K (not shown) showed C1s, N1s, and O1s peaks at 284, 399, and 531 eV, respectively, for **1**, **2**, $[CuL_2(H_2O)_2](NO_3)_2$, $K_2[Ni(CN)_4]$, and $K_2[Pt(CN)_4]$. Thus, the organic ligand moieties, namely, L (lone pair donating amine ligands) and cyanides (well-known π-back-donating ligands), exhibited no remarkable shift of peaks or shake-up of satellite peaks. The $Cu2p_{1/2}$ and $Cu2p_{3/2}$ peaks (Figure 5) are observed at 955.5 and 935.6 eV for **1**, 956.1 and 936.5 eV for **2**, and 956.4 and 936.6 eV for $[CuL_2(H_2O)_2](NO_3)_2$, respectively. The satellite peak, the typical shake-up lines that chemically indicate the Cu^{II} oxidation states, appears around 947 eV. No experimental evidence supporting reduced Cu^{I} states has been reported for the related complexes so far. If a small amount of Cu^{I} ions is contained or mixed, a quite weak peak attributed to the $2p^63d^{10} \rightarrow 2p^53d^{10}4s^1$ transition may be expected to appear at binding energies less than 935 eV.[54,55] The $Ni2p_{1/2}$ and $Ni2p_{3/2}$ peaks (Figure 6) are shown at 858.6 and 876.2 eV for **1** and 859.8 and 877.3 eV for $K_2[Ni(CN)_4]$, respectively. The $Pt4f_{5/2}$, $Pt4f_{7/2}$ (Figure 7a), and $Pt4p_{3/2}$ (Figure 7b) peaks are shown at 79.8, 76.6, and 525.6 eV for **2** and 80.9, 77.5, and 525.8 eV for $K_2[Pt(CN)_4]$, respectively. The spectral shifts of **1** from the precursor $[CuL_2(H_2O)_2](NO_3)_2$ or $K_2[M(CN)_4]$ complexes are relatively larger than those of **2**. Regardless of the extremely bent zigzag chain structures, the electronic distribution and orbital overlap through the cyano bridges of **1** may be stronger than those of **2**, which can be explained by small 3d orbitals of Ni^{II} ions and large 5d orbitals of Pt^{II} ions.[56] The tendency is in agreement with superexchange interactions of magnetic properties (see a later section).

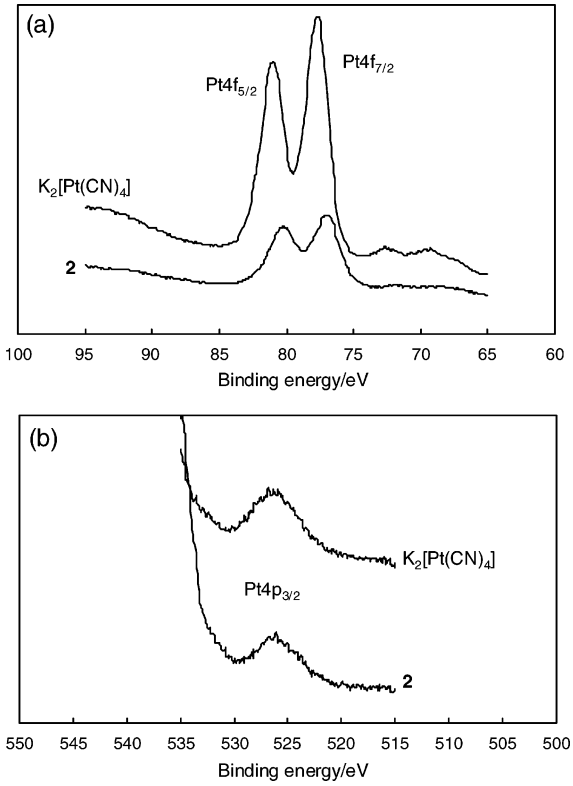

Figure 7. XPS spectra of (a) $Pt4fp_{5/2}$ and $Pt4f_{7/2}$ peaks and (b) $Pt4p_{3/2}$ peaks for **2** and $K_2[Pt(CN)_4]$ at 298 K.

Magnetic Properties. The variable-temperature magnetic susceptibilities of **1** and **2** have been recorded with an applied field of $H = 5000$ G in the temperature range $T = 2-300$ K. Plot of $\chi_M T$ versus T for **1** and **2** are shown in Figures 8 and 9, respectively, where χ_M is the magnetic susceptibility for the $[Cu^{II}L_2][M^{II}(CN)_4]\cdot 2H_2O$ units. The data were analyzed by the Curie−Weiss equation [$\chi_M = C/(T - \theta)$], giving a negative Weiss temperature $\theta = -5.31$ K with $C = 0.319$ cm^3 K mol^{-1} for **1** and $\theta = -5.94$ K with $C = 0.306$ cm^3 K mol^{-1} for **2**. The field dependence of the magnetization ($H = 0-50\,000$ G, $T = 2$ and 5 K) for **1** and **2** are also shown in Figures 8 and 9, respectively. These magnetic behaviors indicate much weaker antiferromagnetic interactions for **1** and **2** than the related cyanide-bridged $Cu^{II}-M^{II}$ complexes.[57] According to their crystal structures, the magnetic orbital of the Cu^{II} ions ($s = 1/2$) is the $d_{x^2-y^2}$

(54) Furlani, C.; Polzonetti, G.; Perti, C.; Tosi, G. *Inorg. Chim. Acta* **1983**, *73*, 105.
(55) Drolet, D. P.; Lees, A. J.; Katnani, A. D. *Inorg. Chim. Acta* **1988**, *150*, 197
(56) Joszai, R.; Beszeda, I.; Benyei, A. C.; Fischer, A.; Kovacs, M.; Maliarik, M.; Nagy, P.; Shchukarev, A.; Toth, I. *Inorg. Chem.* **2005**, *44*, 9643.

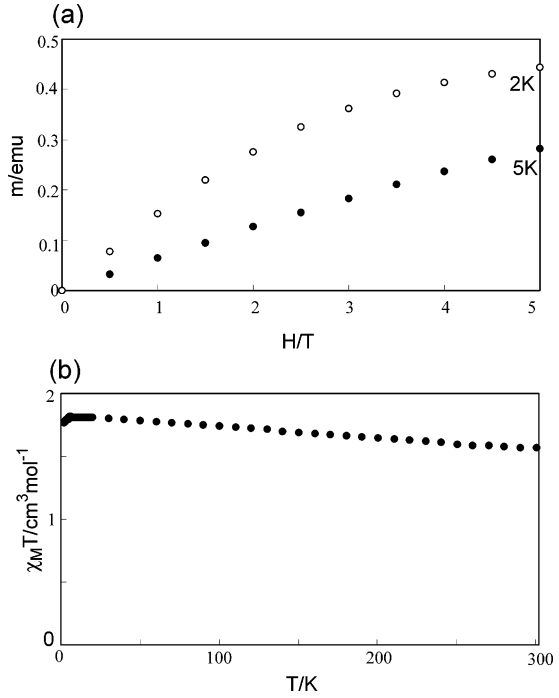

Figure 8. (a) Field dependence of magnetization of **1** at 2 (empty) and 5 K (filled). (b) Plot of the $\chi_M T$ vs T in the range of 2−300 K for **1** at 5000 G.

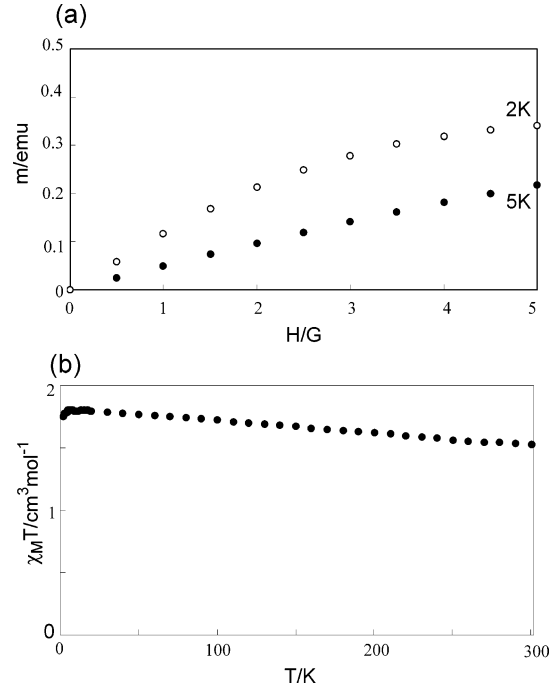

Figure 9. (a) Field dependence of magnetization of **2** at 2 (empty) and 5 K (filled). (b) Plot of the $\chi_M T$ vs T in the range of 2−300 K for **1** at 5000 G.

orbital which is located on the equatorial N−Cu−N axes of the L ligands. Since the overlap of the Ni^{II} ion 3d orbital is stronger than that of the overlap of the Pt^{II} ion 5d orbital, the antiferromagnetic superexchange interaction of **1** may be stronger than that of **2**. Antiferromagnetic interaction may be suggested for both one-dimensional cyanide-bridged chains, but interchain interactions though hydrogen bonds[58] cannot be expected for these complexes. However, the magnetic data are not clear, reflecting the novel structural features of alternating short and long bonds. Antiferromagnetic interaction through short bridges is not weak, while antiferromagnetic interaction through long bridges is quite weak or paramagnetic in character. Therefore, we can give only a tentative interpretation for the magnetic properties.

Conclusion

Two new chiral zigzag one-dimensional cyano-bridged coordination polymers of **1** and **2** are quite characteristic with respect to the asymmetric axial Cu−N(≡C) bond distances. Short axial Cu−N(≡C) bond distances of the one side are 2.324(6) and 2.34(1) Å with Cu−N≡C angles of 137.8(6)° and 138.2(9)° for **1** and **2**, respectively. On the other hand, the long axial Cu−N(≡C) bond distances of the other side are 3.120(8) and 3.09(1) Å with significantly large bent Cu−N≡C bond angles of 97.9(5)° and 96.8(7)° for **1** and **2**, respectively. The asymmetric axial bond distances suggest novel semi-coordination bonds with coexistence of pseudo-Jahn−Teller elongation and long contact via electrostatic interaction of the Cu−N(≡C) bonds forming cyanide-bridged chains. The present case is quite novel in the following points: (1) The axial semi-coordination the Cu−N(≡C) bond distance is quite long for pseudo-Jahn−Teller distortion.[59−61] (2) However, the in-plane L ligands are primary amine exhibiting σ-bonding character, which may form short axial bonds of semi-coordination generally. (3) Nevertheless, the sixth axial coordination atoms (longer cyanide N) are located on the *z*-axis positions, which easily form short bonds with strong electrostatic interaction. (4) Interestingly, two axial Cu−N(≡C) bond distances (the fifth and sixth) are not equivalent, which suggests that (the longer sixth) axial bond exhibits ionic nature. Due to the structures of the cyanide-bridged chains, the characteristic shift of the XPS of $Cu2p_{1/2}$ and $Cu2p_{3/2}$ peaks could be observed for **1**. These complexes also indicate weak antiferromagnetic interaction. However, general consideration of the correlation between structures and electronic states are difficult still, and further studies are necessary for reasonably designing new magneto-optical functional materials.

Acknowledgment. This work was supported by a Grant-in-Aid for the 21st Century COE program 'KEIO Life Conjugate Chemistry' from the Ministry of Education, Culture, Sports, Science, and Technology, Research Foundation for Opto-Science and Technology, and Japan and Mizuho Foundation for the Promotion of Science. The authors are grateful to Professor Tohru Yamada and Dr. Taketo Ikeno (Keio University) for use of the differential scanning calorimetry apparatus, Professor Hidenari Inoue

(57) Cernak, J.; Chomic, J.; Gravereau, P.; Orendacova, A.; Orendac, M.; Kovac, J.; Feher, A.; Kappenstein, C. *Inorg. Chim. Acta* **1988**, *281*, 134.
(58) Ghoshal, D.; Ghosh, A. K.; Maji, T. K.; Ribas, J.; Mostafa, G.; Zangrando, E.; Chaudhuri, N. R. *Inorg. Chim. Acta* **2006**, *359*, 593.
(59) Hathaway, B. J.; Biling, D. E. *Coord. Chem. Rev.* **1970**, *5*, 143.
(60) Hathaway, B. J. *Struct. Bonding (Berlin)* **1973**, *14*, 49.
(61) Hathaway, B. J. *Struct. Bonding (Berlin)* **1984**, *57*, 55.

(Keio University) for use of the CD/MCD spectrometer, and Professor Katsuya Inoue, Dr. Motoko Akita-Tanaka, and Dr. Junichi Nishijo (Institute for Molecular Science) and Mr. Isamu Oguro (Institute for Solid State Physics, University of Tokyo) for use of the SQUID facility.

Supporting Information Available: X-ray crystallographic file, in CIF format, for structural determination of the title compounds. This material is available free of charge via the Internet at http://pubs.acs.org.

IC060783A